



HAL
open science

An investigation of the performances of asynchronous measurements methods

Nathan Itare, Gilles Chardon, José Picheral

► **To cite this version:**

Nathan Itare, Gilles Chardon, José Picheral. An investigation of the performances of asynchronous measurements methods. Inter-Noise 2024, Aug 2024, Nantes, France. pp.8806-8815, 10.3397/IN_2024_4146 . hal-04735374

HAL Id: hal-04735374

<https://hal.science/hal-04735374v1>

Submitted on 14 Oct 2024

HAL is a multi-disciplinary open access archive for the deposit and dissemination of scientific research documents, whether they are published or not. The documents may come from teaching and research institutions in France or abroad, or from public or private research centers.

L'archive ouverte pluridisciplinaire **HAL**, est destinée au dépôt et à la diffusion de documents scientifiques de niveau recherche, publiés ou non, émanant des établissements d'enseignement et de recherche français ou étrangers, des laboratoires publics ou privés.



An investigation of the performances of asynchronous measurements methods

Nathan Itare¹

Université Paris-Saclay, CNRS, CentraleSupélec, Laboratoire des signaux et systèmes
91190, Gif-sur-Yvette, France

Gilles Chardon²

Université Paris-Saclay, CNRS, CentraleSupélec, Laboratoire des signaux et systèmes
91190, Gif-sur-Yvette, France

José Picheral³

Université Paris-Saclay, CNRS, CentraleSupélec, Laboratoire des signaux et systèmes
91190, Gif-sur-Yvette, France

ABSTRACT

In acoustical imaging and source localization, several methods for the exploitation of asynchronous array measurements have been proposed, based on covariance matrix completion, Bayesian estimation, fusion of beamforming maps, etc. The goal of asynchronous measurements is to reach the performance of large and dense arrays, with reduced experimental effort, by moving an array of limited size between experiments, and fuse the obtained data to produce an estimation of the distribution of acoustical sources. In this study, we consider the performances that one can expect from asynchronous measurements, and investigate the actual performances of several methods from the state of the art. In particular, the mean squared errors of the estimation of the position and power of an acoustical source are estimated using simulations and experimental measurements.

1. INTRODUCTION

To address the limitation of arrays of limited aperture or low density, many studies have explored using a single microphone array sequentially moved to different locations. This approach yields non-synchronized measurements from multiple subarrays, with each subarray corresponding to the physical array in a different position. These measurements, called *asynchronous measurements*, can be processed in different ways. Such measurements are expected to extend the frequency range of the array and/or the imaging region.

There are mainly two types of approaches to process asynchronous measurements: the first is to process the data from each subarray separately (e.g. by computing a beamforming map), and combining the obtained results [1, 2], and the second aims to first estimate a full covariance matrix,

¹nathan.itare@centralesupelec.fr

²gilles.chardon@centralesupelec.fr

³jose.picheral@centralesupelec.fr

as if the measurements had been obtained synchronously. In the case of asynchronous measurements, the challenge arises from the lack of information to determine the inter-array covariance matrices, as only the subarray data covariance matrix can be estimated. The completion of the full data covariance matrix can be attempted using *reference microphones* that have a fixed position between successive measurement [3]. Another technique was introduced in Antoni *et al.* [4], which enables to reconstruct the sound field without the use of reference microphones. Several algorithms were then developed using a similar approach. These algorithms enable to solve a low rank minimization of the full covariance matrix combined with the fitting of individual covariance matrices estimated for each measurement. First, cyclic projection (CP) was proposed [5], followed by the fast iterative soft threshold algorithm (FISTA) [6]. Faster algorithms were proposed using augmented Lagrange multiplier (ALM) or alternating direction method of multipliers (ADMM) [7] and other variants were also studied [8, 9]. Finally, another approach was investigated to complete the full data covariance matrix: the block hermitian matrix completion method (BHMC) proposed in [10] is based on the low rank and Hermitian properties of the covariance matrix.

The aim of this study is to investigate the performances of these methods, in particular in terms of the mean squared error (MSE) of the estimation of the position and power of a source. This is a first step towards a quantitative assessment of asynchronous array methods for source localization. Quantitative evaluation of asynchronous methods were already performed, however involving the covariance matrix completion error, which is not relevant for methods not based on matrix completion, or the reconstruction error of smooth distributions of sources.

We focus on two completion approaches to process asynchronous measurements : the BHMC method [10] and an optimized fast iteration algorithm using ADMM, exploiting continuity constraints on the acoustical field proposed in [7]. In addition, this paper also considers maximum likelihood estimation (MLE) and the arithmetic averaging of beamforming maps obtained by each subarray, approximating a variant of MLE where the power of the source can vary between measurements [11]. Three array scenarios are considered: contiguous, interlaced and overlapped arrays. This paper is organized as follows: Section 2 describes the asynchronous measurements' principle. Section 3 presents the two covariance matrix completion techniques. Simulation results are presented in section 4. Section 5 shows experimental results, and Section 6 is the conclusion.

2. ASYNCHRONOUS MEASUREMENTS PRINCIPLE

This section introduces a statistical model for asynchronous measurements, presents three scenarios for the configuration of the measurements, and finally discuss the Cramér-Rao bounds for these scenarios.

2.1. Model

Acoustic measurements are acquired asynchronously using J subarrays. For the sake of simplicity, we assume that these subarrays have the same number of microphones M , and the measurement duration is equal for each array. In practice, the J subarrays can be obtained with only one physical array which is moved to different positions. The temporal acoustical measurements are analyzed by a short time Fourier transform, yielding S snapshots. For a given frequency f and K sources, the measured data acquired at the j^{th} subarray and at the s^{th} snapshot can be expressed as:

$$\mathbf{p}_{js} = \sum_{k=1}^K a_{kjs} \mathbf{g}_j(\mathbf{x}_k) + \mathbf{n}_{js}. \quad (1)$$

where the a_{kjs} are the complex amplitudes of source k in each frame j , \mathbf{n}_{js} is the measurement noise supposed to be white in space and in time. $\mathbf{g}_j(\mathbf{x}_k)$ is the Green function vector between the source

placed in \mathbf{x}_k and the microphones of the j^{th} subarray. In free field propagation,

$$\mathbf{g}_j(\mathbf{x}) = \frac{\exp(-i\kappa\|\mathbf{x} - \mathbf{y}_j\|_2)}{\|\mathbf{x} - \mathbf{y}_j\|_2}, \quad (2)$$

with κ being the wave-number corresponding to the frequency of interest f , and \mathbf{y}_j the position of the microphones for the j^{th} subarray. Note that the analysis proposed here does not make any assumption on the Green function.

In the methods considered here, the complex amplitudes a_{kjs} are assumed to be random. More precisely, the amplitudes a_{kjs} of the k -th source are drawn from the complex circular normal distribution [12] with zero mean and variance p_k , the power of source. For each subarray j , the theoretical covariance matrix of the measurements is:

$$\Sigma_j(\theta) = \mathbb{E}(\mathbf{p}_{js}\mathbf{p}_{js}^H) = \sum_{k=1}^K p_k \mathbf{g}_j(\mathbf{x}_k)\mathbf{g}_j(\mathbf{x}_k)^H + \sigma^2 \mathbf{I}, \quad (3)$$

where θ is the vector of parameters to be estimated containing the positions \mathbf{x}_k and powers p_k of the sources, $\mathbb{E}(\cdot)$ is the mathematical expectation.

The Sample Covariance Matrice (SCM) (or cross-spectral matrices) of the j^{th} subarray is estimated from the measurements by:

$$\hat{\Sigma}_j = \frac{1}{S} \sum_{s=1}^S \mathbf{p}_{js}\mathbf{p}_{js}^H. \quad (4)$$

2.2. Microphone array configurations

We consider a single physical uniform linear array with 8 microphones, and the data are generated from two asynchronous measurements, where the second measurement corresponds to a shift of the physical array. Localization performance will be evaluated across three classical scenarios found in the literature [4, 5]. These scenarios are depicted in Figure 1, where subarray 1 corresponds to the first measurement, and subarray 2 pertains to the second measurement.

In the first scenario, the physical array is shifted by the aperture length, aligning the two subarrays adjacently. In the second scenario, the two subarrays are interleaved, and in the last scenario, the two subarrays overlap to include two reference microphones. The inter-sensor distance of the physical array is 8 cm for scenarios 1 and 3, while it is 16 cm for scenario 2.

2.3. Cramér-Rao Bounds

The Cramér-Rao bound (CRB) is a lower bound on the variance of all unbiased estimators of the parameters of a statistical model. Here, we consider the CRBs of the estimation of the position and power of a source, which can be easily computed [11], for the three array configurations introduced above. The CRB can be used to compare the performance that are to be expected for the three configurations.

CRB are evaluated for a wave-number $\kappa = 10 \text{ m}^{-1}$ with sources power and a noise power of 1 Pa². The distance between the array and the source is 1.5 m.

CRBs are plotted in Figure 2 for various source positions (in the \vec{x} axis). For each scenario, the CRB is evaluated for both synchronous and asynchronous cases. In the synchronous case, where both subarrays acquire data simultaneously, the number of samples is twice that of each asynchronous measurement, in order to maintain the same total measurement time.

As expected, synchronous arrays demonstrate the best performances compared to non-synchronous arrays. For asynchronous measurements, the scenario 2 (with the interleaved array) exhibits the best performance. Indeed, for this configuration, the aperture of the subarrays is similar

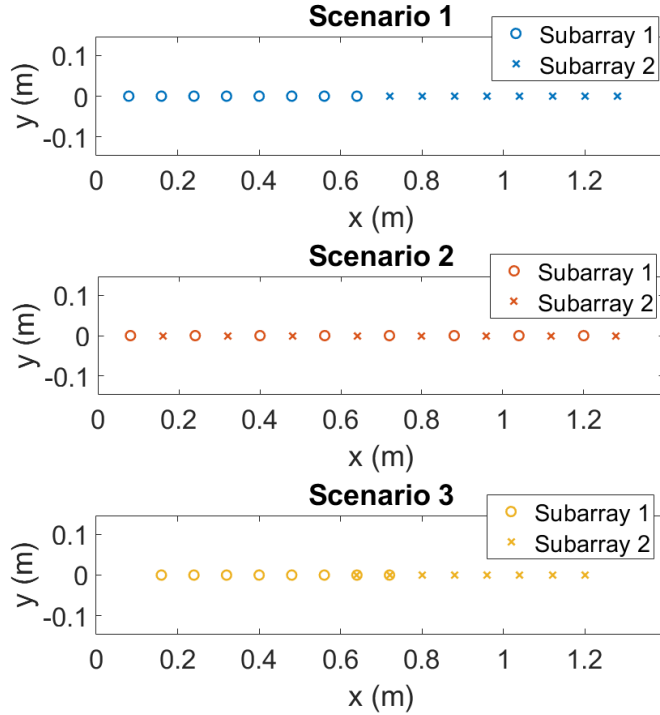


Figure 1: Position of the microphones for the asynchronous measurements for three scenarios. The rounds correspond to the first measurement and the crosses to the second measurement.

to the aperture of the complete array. In the overlapped case, the presence of common reference microphones between the two subarrays does not significantly impact the CRB.

Figure 3 shows the CRB for the first scenario compared to the CRB of the two subarrays used independently. When sources are positioned roughly in front of the center of the subarrays, performances are better using the measurement of this subarray than using both asynchronous measurements. However, in practice, the position of the source is not known before the measurements, and thus it is impossible to select the subarray that would provide the best performance.

From the analysis of the CRB, we can conclude that while asynchronous arrays cannot reach the performances of the complete synchronous array, they may be beneficial to the performances compared to single arrays. Indeed, the maximum CRBs with respect to the source position is lower than that of the elementary synchronous arrays considered separately.

3. MAXIMUM LIKELIHOOD BASED METHODS

Given data and a statistical model for the data (usually, Gaussian sources and noise), the parameters of the source can be estimated by maximum likelihood estimation (MLE). In the case of a unique source, beamforming was shown to be an instance of MLE [13].

In [11], MLE was considered for the localization of a unique source using asynchronous measurements. In cases where the power of the source is assumed to be constant for every measurement, as in (3), the position and the power of the source are jointly estimated by solving the optimization problem:

$$(\hat{\mathbf{x}}, \hat{p}) = \underset{\mathbf{x} \in \Omega, p \in \mathbf{R}_+}{\operatorname{argmin}} \sum_{j=1}^J S_j \left(-\frac{p \mathbf{g}_j(\mathbf{x})^H \hat{\Sigma}_j \mathbf{g}_j(\mathbf{x})}{\sigma^2 (\sigma^2 + p \|\mathbf{g}_j(\mathbf{x})\|^2)} + \log(\sigma^2 + p \|\mathbf{g}_j(\mathbf{x})\|^2) \right) \quad (5)$$

In a relaxed model, where the power of the source is allowed to change between measurements,

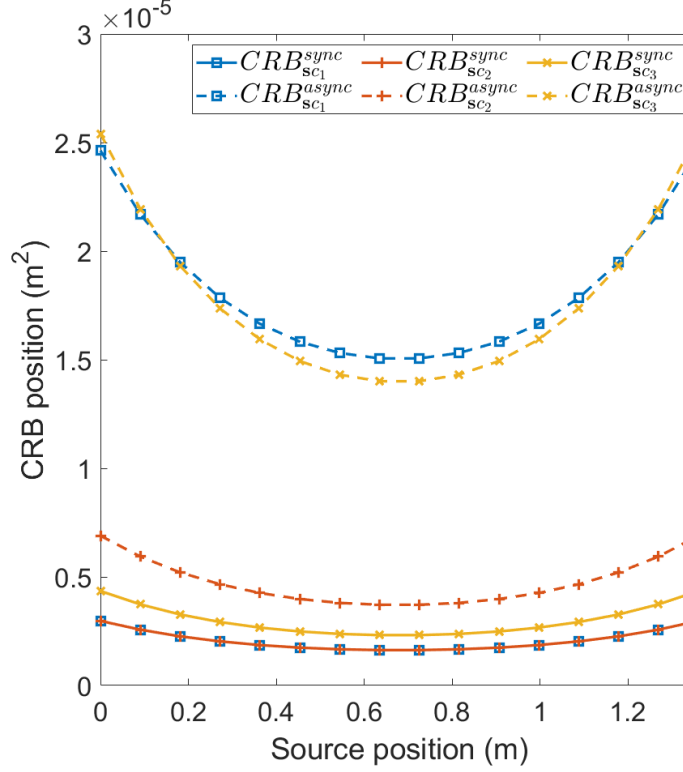


Figure 2: CRB for $\kappa = 10 \text{ m}^{-1}$, for different source positions, in the synchronous and asynchronous cases. Blue squares, red plus and yellow crosses correspond respectively to the first, second and third scenarios.

the position is estimated by maximizing the sum of the beamforming criteria computed for each subarray:

$$B(\mathbf{x}) = \sum_{j=1}^J S_j \left(\frac{\mathbf{g}_j(\mathbf{x})^H \hat{\Sigma}_j \mathbf{g}_j(\mathbf{x})}{\|\mathbf{g}_j(\mathbf{x})\|^2 \sigma^2} - \log \frac{\mathbf{g}_j(\mathbf{x})^H \hat{\Sigma}_j \mathbf{g}_j(\mathbf{x})}{\|\mathbf{g}_j(\mathbf{x})\|^2 \sigma^2} \right) \quad (6)$$

In the cases presented here, the log term can be neglected since it doesn't bring significant changes to the estimations. This method is called Σ BF in the following of the paper. This fusion method by arithmetic averaging was considered in [14] and [1].

4. COVARIANCE MATRIX COMPLETION TECHNIQUES

In covariance matrix completion techniques, the full covariance matrix is first estimated to approximate the covariance matrix that we would obtain if the measurements were made using a synchronous array. This completed matrix is then used as input to a standard source localization method. These matrix completion methods are based on the estimation of low-rank matrices, with the optional addition of soundfield continuity constraints.

4.1. Block Hermitian Matrix Completion

BHMC [10] estimates a complete SCM under the assumption that the number of sources is small compared to the dimension of the SCM, and that the contribution of the noise to the SCM is negligible. In this case, the complete SCM has a low rank.

The estimated complete SCM is found by solving the following problem:

$$\text{minimize } \text{rank}(\hat{\Sigma}^c) \text{ subject to } \mathcal{A}(\hat{\Sigma}^c) = \hat{\Sigma}^m, \quad (7)$$

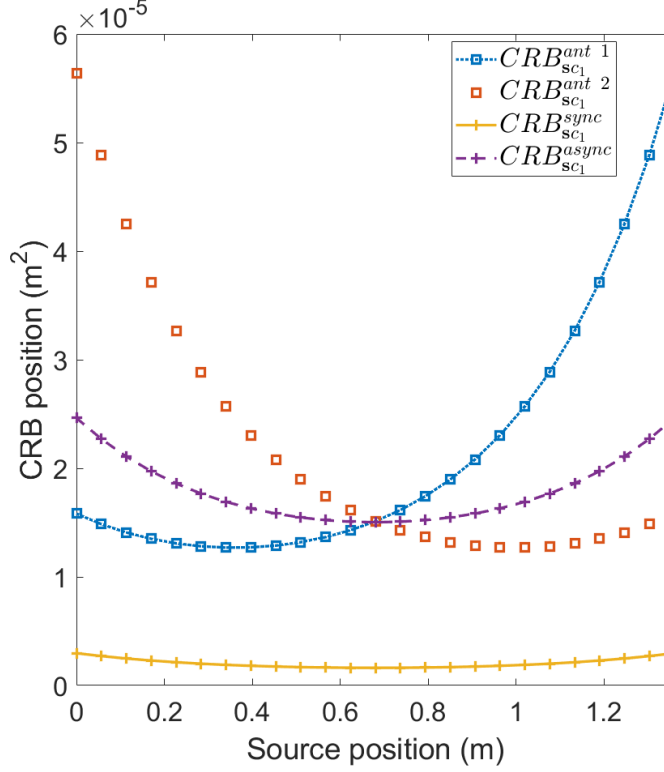


Figure 3: CRBs for $\kappa = 10 \text{ m}^{-1}$, for different source positions and in the first scenario.

with $\hat{\Sigma}^c$ the estimated full matrix, $\hat{\Sigma}^m$ a matrix containing all the partial covariance matrix $\hat{\Sigma}_j$ in diagonal blocks, and $\mathcal{A} : \mathbb{C}^{MJ \times MJ} \rightarrow \mathbb{C}^{MJ \times MJ}$ an operator that set to zero the elements out of the $M \times M$ diagonal blocks. The minimization problem is solved non-iteratively by the algorithm given in [10].

This method cannot be expected to yield accurate results. Indeed, the optimization problem (7) on which BHMC is based is not capable of recovering the phase relationship between the subarrays [5], as the phases of the diagonal blocks are non-uniquely defined. In the particular case of two subarrays, we have the following result: let

$$\mathbf{M}_0 = \begin{pmatrix} \mathbf{A} & \mathbf{C}^* \\ \mathbf{C} & \mathbf{B} \end{pmatrix} \text{ and } \mathbf{M}_\psi = \begin{pmatrix} \mathbf{A} & e^{i\psi} \mathbf{C}^* \\ e^{-i\psi} \mathbf{C} & \mathbf{B} \end{pmatrix}, \quad (8)$$

with \mathbf{M}_0 semi-definite positive. Then $\forall \psi$, \mathbf{M}_ψ is semi-definite positive and has the same rank as \mathbf{M}_0 . This is a direct consequence of the equality:

$$\mathbf{M}_\psi = \begin{pmatrix} \mathbf{I} & \mathbf{0} \\ \mathbf{0} & e^{-i\psi} \mathbf{I} \end{pmatrix} \mathbf{M}_0 \begin{pmatrix} \mathbf{I} & \mathbf{0} \\ \mathbf{0} & e^{i\psi} \mathbf{I} \end{pmatrix}. \quad (9)$$

4.2. Soundfield continuity based methods

Methods based on the continuity of the soundfield add the constraint that the complete covariance matrix should be representative of a soundfield compatible with the relative placement of the subarrays and the sources. As an example, the completed covariance matrix can be recovered by the optimization problem [7]:

$$\underset{\hat{\Sigma}^c}{\text{minimize}} \lambda \|\hat{\Sigma}^c\|_* + \frac{1}{2} \|\mathcal{A}(\hat{\Sigma}^c) - \hat{\Sigma}^m\|_F^2 \text{ subject to } \hat{\Sigma}^c \geq 0 \text{ and } \|\hat{\Sigma}^c - \Psi \hat{\Sigma}^c \Psi^H\|_2^2 \leq \epsilon, \quad (10)$$

with λ being a regularization parameter which balances the partial covariance matrix fitting term and the rank minimization term. The constraint $\|\hat{\Sigma}^c - \Psi \hat{\Sigma}^c \Psi^H\|_2^2 \leq \epsilon$ enforces the continuity of the soundfield, where Ψ is the projection matrix onto a small dimension space, e.g., the space spanned by the first K singular values of the propagation matrix.

The addition of the field continuity terms is expected to alleviate the non-uniqueness problems encountered in BHMC. In this paper, we will consider the ADMM based approach of [7] that we will call Soundfield Continuity Matrix Completion (SCMC). For the projection basis, a singular value decomposition of the steering matrix \mathbf{D} (containing all the green functions between the grid sources and the microphone) is performed, $\mathbf{D} = \mathbf{U}_D \Sigma_D \mathbf{V}_D^*$. Then N_p singular vectors of \mathbf{U}_D are selected to form the projection basis such as $\Psi = \mathbf{U}_{N_p} \mathbf{U}_{N_p}^H$.

5. NUMERICAL RESULTS

Numerical simulations are performed in the three scenarios to evaluate the performances of BHMC and SCMC compared to the MLE defined in eq. (5), and to the averaged beamforming Σ BF. In addition, the performance of beamforming with synchronous measurements is also considered.

MSE are first estimated, simulating fifty trials with 5000 snapshots, the source at position (0.73, 1.5) m and a signal-to-noise ratio (SNR) of 0.9 dB. The parameters for SCMC are the same as in [7] except for the positive penalty parameter $\mu=0.5$ and the number of singular vectors chosen $N_p = 10$. The value of μ is set to minimize the mean of MSEs obtained for the three scenarios with one source.

Figure 4 presents the MSE for the five methods. The results show that beamforming with synchronous arrays gives the better performance in all cases as expected. In the three scenarios, Σ BF and MLE give better results compared to other asynchronous methods, with a better performance of MLE in low frequency. In the second scenario, there is a small gap between the synchronous beamforming and the asynchronous methods, which confirms that this measurement scenario is better.

SCMC is on average close to Σ BF in all three scenarios. BHMC shows high errors in most frequencies in the three scenarios, such that not all errors are visible in the figure.

These results confirm that BHMC, which results are arbitrarily dependent on the numerical algorithm used to compute the eigenvectors of the SCMs, cannot estimate the position of the source accurately. Comparing SCMC and the averaged beamforming Σ BF, SCMC does not exhibit better performance than the averaged beamforming Σ BF which has also the lower computational cost.

6. EXPERIMENTAL RESULTS

Experiments have been conducted to compare with the results obtained in simulation. Array geometries and scenarios are the same as those presented in section 2. The source is a white noise emitted with a baffled Visaton-BF32 loudspeaker. The microphone used are MEMS microphones (INVENSENSE - INMP441). Measurements were performed in an anechoic room.

MSE are first evaluated in function of the frequency. The source is placed at 1.5 m from the array and at 0.73 m in the x-axis, and noise is added after the measurements such that the SNR is around 0.78 dB. Signals are acquired 60 times each during around 5 s to estimate the MSE, with a sampling frequency of 20 kHz.

Results are presented in Figure 5. As in the simulations, BHMC gives higher MSE than all the other methods for most of the frequencies. The decrease in MSE with frequency is visible, and the synchronous beamforming performs better than asynchronous methods. The gap between synchronous beamforming and asynchronous methods (MLE and Σ BF) in the first and last scenario is present as for the simulation, and the closeness between the three methods in the second scenario is also visible. Conclusions consistent with the simulation results are reached, with good performances of Σ BF compared to SCMC and BHMC.

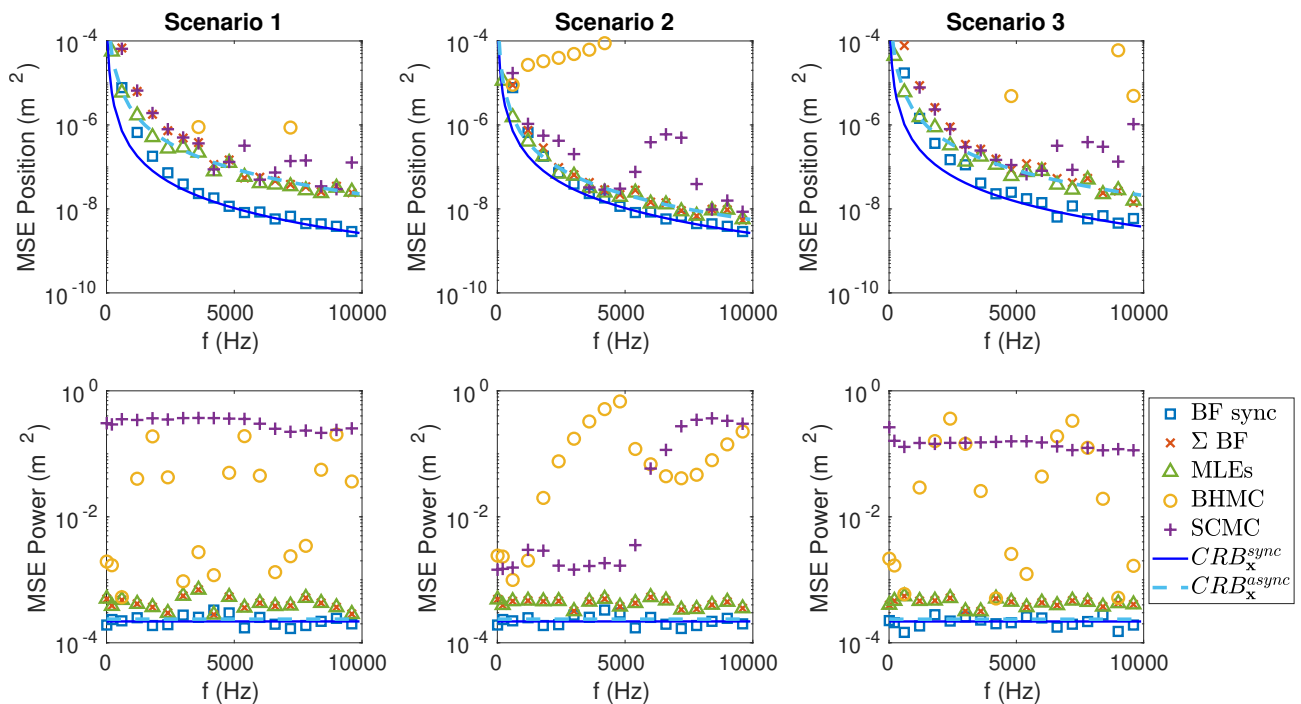


Figure 4: Experimental results: MSE and CRB vs frequency for the five methods presented, for the position (top) and power (bottom) of the source.

7. CONCLUSION

This study investigated different methods to process asynchronous measurements. While they do not reach the performances of synchronous measurements, asynchronous measurements are beneficial to the performances of source localization compared to the use of a unique array, keeping the total duration of the experiment constant, as shown by computing the CRBs for the estimation of the parameters of the sources.

Simulations and experiments results show that in all the studied cases, completing the full covariance matrix is not necessary to obtain accurate source localization results. In particular, the simulations showed that simpler methods such as MLE and Σ BF reach the CRBs, a lower bounds on the MSE of the estimation of the position and power of the source.

We note that matrix completion methods combined with beamforming have a higher computational cost than Σ BF, as the computational complexity of computing a beamforming map of L points is LJM^2 for Σ BF, and LJ^2M^2 for beamforming after completion, to which the computational complexity of the completion matrix should be added.

From these results, obtained for source localization by beamforming, we formulate the hypothesis that, in general, asynchronous arrays data can be processed without completing a full matrix without degrading localization performances, keeping the computational demands limited due to the smaller data to be processed. This conjecture, of course, remains to be tested on more general source localisation settings.

REFERENCES

1. Lourenço Tércio Lima Pereira, Roberto Merino-Martínez, Daniele Ragni, David Gómez-Ariza, and Mirjam Snellen. Combining asynchronous microphone array measurements for enhanced acoustic imaging and volumetric source mapping. *Applied Acoustics*, 182:108247, November 2021.
2. Wassim Suleiman, Pouyan Parvazi, Marius Pesavento, and Abdelhak M. Zoubir. Non-Coherent

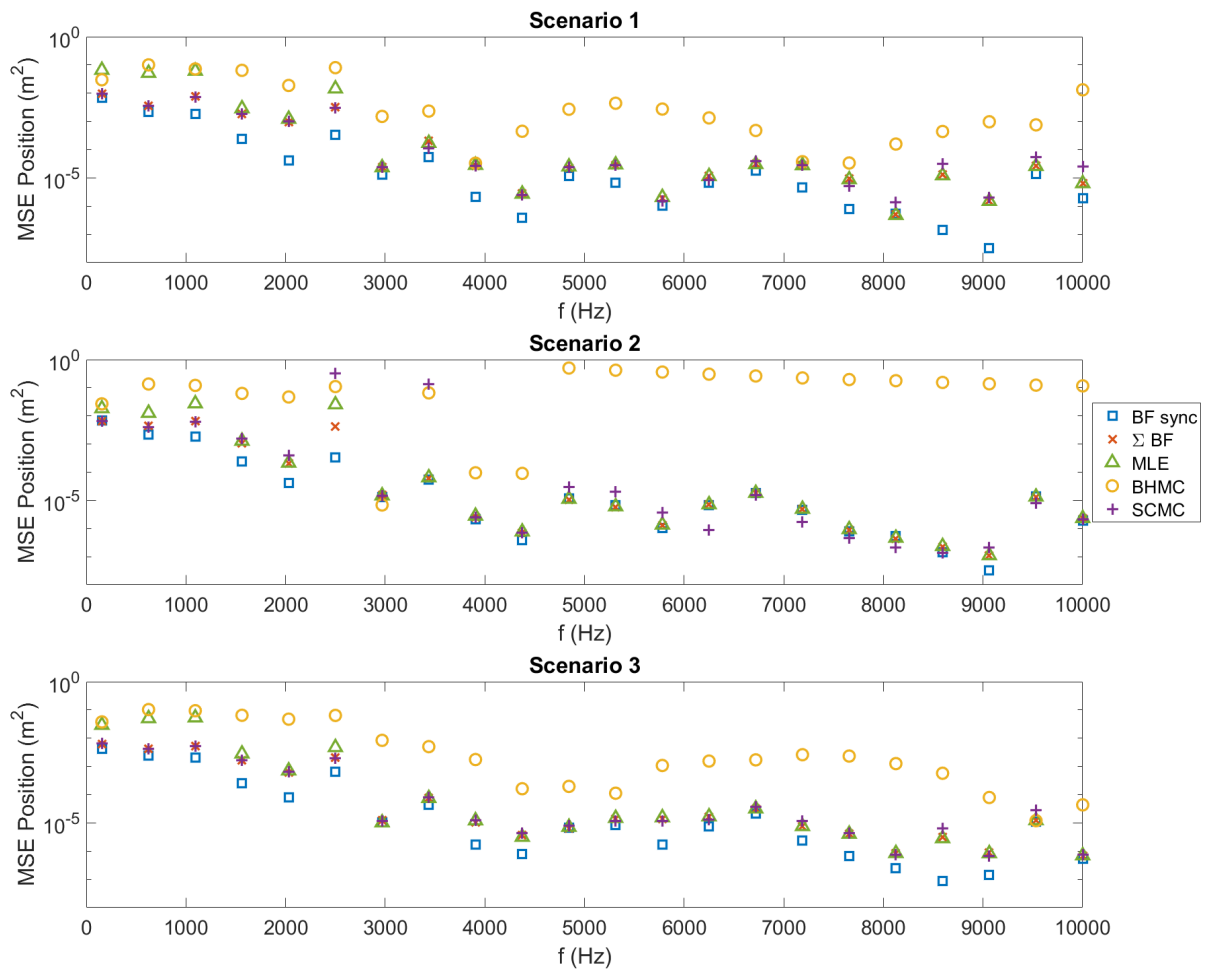


Figure 5: Experimental results: MSE vs frequency for the five methods presented.

Direction-of-Arrival Estimation Using Partly Calibrated Arrays. *IEEE Transactions on Signal Processing*, 66(21):5776–5788, November 2018.

3. S.H. Yoon and P.A. Nelson. A method for the efficient construction of acoustic pressure cross-spectral matrices. *Journal of Sound and Vibration*, 233(5):897–920, June 2000.
4. Jerome Antoni, Yu Liang, and Quentin Leclère. Reconstruction of sound quadratic properties from non-synchronous measurements with insufficient or without references: Proof of concept. *Journal of Sound and Vibration*, 349:123–149, August 2015.
5. Liang Yu, Jerome Antoni, and Quentin Leclere. Spectral matrix completion by Cyclic Projection and application to sound source reconstruction from non-synchronous measurements. *Journal of Sound and Vibration*, 372:31–49, June 2016.
6. Liang Yu, Jerome Antoni, Quentin Leclere, and Weikang Jiang. Acoustical source reconstruction from non-synchronous sequential measurements by Fast Iterative Shrinkage Thresholding Algorithm. *Journal of Sound and Vibration*, 408:351–367, November 2017.
7. Liang Yu, Jerome Antoni, Haijun Wu, Quentin Leclere, and Weikang Jiang. Fast iteration algorithms for implementing the acoustic beamforming of non-synchronous measurements. *Mechanical Systems and Signal Processing*, 134:106309, December 2019.
8. Fangli Ning, Jinglong Hu, Hongjie Hou, Keqiang Yao, Juan Wei, and Baoqing Li. Sound source localization of non-synchronous measurements beamforming based on the truncated nuclear norm regularization. *Applied Acoustics*, 191:108688, March 2022.
9. Lin Chen, Youhong Xiao, Liang Yu, and Tiejun Yang. Algorithms with randomization-based acceleration strategies for sound source localization by non-synchronous measurements.

Mechanical Systems and Signal Processing, 188:109996, April 2023.

10. Fangli Ning, Jiahao Song, Jinglong Hu, and Juan Wei. Sound source localization of non-synchronous measurements beamforming with block Hermitian matrix completion. *Mechanical Systems and Signal Processing*, 147:107118, January 2021.
11. Gilles Chardon. Maximum likelihood estimators and cramer-rao bounds for the localization of an acoustical source with asynchronous arrays. *Journal of Sound and Vibration*, 565:117906, 2023.
12. B. Picinbono. Second-order complex random vectors and normal distributions. *IEEE Transactions on Signal Processing*, 44(10):2637–2640, October 1996. Conference Name: IEEE Transactions on Signal Processing.
13. Gilles Chardon. Theoretical analysis of beamforming steering vector formulations for acoustic source localization. *Journal of Sound and Vibration*, 517:116544, 2022.
14. Paolo Castellini and Andrea Sassaroli. Acoustic source localization in a reverberant environment by average beamforming. *Mechanical Systems and Signal Processing*, 24(3):796–808, April 2010.